ERDC/GSL TR-21-30

Geotechnical and Structures Laboratory

US Army Corps of Engineers®
Engineer Research and Development Center

ERDC
ENGINEER RESEARCH & DEVELOPMENT CENTER

Land-based and Water-borne Ground Penetrating Radar Surveys – Interim Report

Geophysical Investigation to Assess Condition of Grouted Scour Hole

Old River Control Complex—Low Sill Concordia Parish, Louisiana

Janet E. Simms, Benjamin R. Breland, and William E. Doll

September 2021

ERDC/GSL TR-21-30
September 2021

Geophysical Investigation to Assess Condition of Grouted Scour Hole

Old River Control Complex—Low Sill Concordia Parish, Louisiana

Janet E. Simms and Benjamin R. Breland

Geotechnical and Structures Laboratory
U.S. Army Engineer Research and Development Center
3909 Halls Ferry Road
Vicksburg, MS 39180-6199

William E. Doll

Oak Ridge Institute for Science and Education
P.O. Box 117
Oak Ridge, TN 37831-0117

Final report

Prepared for U.S. Army Corps of Engineers
New Orleans District
7400 Leake St.
New Orleans, LA 70118

Under Funding provided by the sponsoring agency

Abstract

Geophysical surveys, both land-based and water-borne, were conducted at the Old River Control Complex–Low Sill, Concordia Parish, LA. The purpose of the surveys was to assess the condition of the grout within the scour region resulting from the 1973 flood event, including identification of potential voids within the grout. Information from the ground studies will also be used for calibration of subsequent marine geophysical data and used in stability analysis studies. The water-borne survey consisted of towed low frequency (16-80 MHz) ground penetrating radar (GPR), whereas the land-based surveys used electrical resistivity and seismic refraction. The GPR survey was conducted in the Old River Channel on the upstream side of the Low Sill structure. The high electrical conductivity of the water (~50 mS/m) precluded penetration of the GPR signal; thus, no useful data were obtained. The land-based surveys were performed on both northeast and southeast sides of the Low Sill structure. Both resistivity and seismic surveys identify a layered subsurface stratigraphy that corresponds, in general, with available borehole data and constructed geologic profiles. In addition, an anomalous area on the southeast side was identified that warrants future investigation and monitoring.

Contents

Figures and Table

Figures

Table

Preface

This study was conducted for the U.S. Army Corps of Engineers (USACE), New Orleans District (MVN), under funding provided by the sponsor. The technical monitor was Dr. Maureen K. Corcoran.

The work was performed by the Geotechnical Engineering and Geosciences Branch (GSG) of the Geosciences and Structures Division (GSD), U.S. Army Engineer Research and Development Center, Geotechnical and Structures Laboratory (ERDC-GSL). At the time of publication, Mr. Christopher G. Price was Chief, GSG; and Mr. James L. Davis was Chief, GS. The Deputy Director of ERDC-GSL was Mr. Charles W. Ertle II, and the Director was Mr. Bartley P. Durst.

COL Teresa A. Schlosser was the Commander of ERDC, and Dr. David W. Pittman was the Director.

The New Orleans District points of contact are Ms. Jean Vossen and Mr. David Ramirez, CEMVN-ED-H, Mr. Craig B. Waugaman, CEMVN-EDS, and Mr. Jeffrey J. Varisco, CEMVN-PPPMD; the Morganza Project Office point of contact is Mr. Russell Beauvais, CEMVN-OD-J; and the Low Sill Project Office point of contact is Mr. Stacey Hodnett, CEMVN-OD-JO.

The authors greatly appreciate the assistance provided by the Low Sill Project Office. Special thanks to Mr. P. Scott Lartigue, CEMVN-OD, who expertly captained the boat during the GPR surveys. His knowledge of the channel, structure history, and suggestions contributed to a successful deployment of the water-borne GPR system. Without the support of all Low Sill personnel, the geophysical investigation could not have been completed within the allotted time.

1 Introduction

The U.S. Army Engineer Research and Development Center (ERDC) was tasked by the U.S. Army Corps of Engineers (USACE), New Orleans District (MVN), with assessing the condition of a grouted scour hole located at the southeast wall of Low Sill at the Old River Control Complex (ORCC), Concordia Parish, LA. One phase of this effort involves both land-based and water-borne geophysical surveys led by the ERDC Geotechnical Engineering and Geosciences Branch (GEGB). Geophysical techniques are non-invasive, cover greater spatial area than invasive methods, and can generally be performed in less time and at lower cost than invasive methods. Geophysical investigations have been designed to assess the condition of the grout to include delineation of the boundaries of the grout body and riprap fill volume and identification of anomalies within the grout/riprap body that might be associated with voids or similar areas of concern. Because the scour hole and fill materials are largely confined to the channel, they must be assessed with water-borne geophysical surveys. Field work is being conducted in two phases. In autumn 2018, a marine ground penetrating radar (GPR) survey 10-14 September and a land-based data collection 29 October to 2 November were conducted. Because it is unsafe to acquire marine data while the floodgates are open, it was not possible to deploy either the marine seismic or resistivity geophysical systems in the autumn of 2018. A second phase, consisting of both marine seismic and resistivity surveys, was to be planned once water levels subside. This report provides a description and analysis of data that were acquired in 2018.

The purpose of the 2018 water-borne GPR survey was to identify potential void areas within the grouted scour region. Land-based seismic refraction and resistivity surveys were conducted to assess subsurface structural features adjacent to the scour volume for two purposes:

1. To define the geophysical properties, including seismic velocities and electrical resistivities as well as their lateral continuity for comparison with geologic cross sections (Breland et al. 2021*), and for calibration of the subsequent marine geophysical data, and
2. To identify voids, soil transitions, or other features in proximity to the dam structure that might influence the long-term stability of the ORCC–Low Sill.

The Old River Control Complex, authorized by the Flood Control Act of 1954, Public Law (PL) 780 under the 83rd Congress, is located approximately 35 miles south of Natchez, MS, and 48 miles northwest of Baton Rouge, LA, along the west bank of the Mississippi River between river miles 317 and 311 in Concordia Parish (Figure 1). The ORCC consists of four primary structures, i.e., Low Sill Structure (Low Sill), Overbank Control Structure (Overbank), Auxiliary Structure (Auxiliary), and the Sidney A. Murray Hydroelectric Station. The complex also includes a navigation lock, both forebay and tail-bay channels, an earthen dam closing the Old River, main-line levee extensions, and bank stabilization along the Red and Atchafalaya rivers.

The Low Sill Control Structure (LSCS) was constructed between 1955 and 1958, along with the Overbank, to prevent a natural cutoff from occurring from the Mississippi River into the Atchafalaya River. The Auxiliary was constructed (ca. 1986) to aid in reducing the flow of water through the existing structures yet still allow the Corps to maintain the distribution of flow. The Low Sill and Overbank structures work together with the Auxiliary and Sidney A. Murray Hydroelectric Station (ca. 1990) to maintain a 30-percent flow diversion from the Mississippi River into the Atchafalaya River.

During the Flood of 1973, an eddy current produced a scour hole, proximal to the southeast upstream left wing wall, approximately 300.0 ft in diameter with a maximum depth of 60.0 ft. Emergency repairs of Low Sill were conducted by riprap placement and grouting of the scour hole using several mixtures of low-cement, low-bond strength grout.

* Breland, B. R., L. A. Walshire, J. R. Kelley, D. W. Harrelson, M. K. Corcoran, M. Zakikhani, J. E. Simms. 2021. *Old River Control Complex (ORCC) Low Sill: A literature synthesis.* Draft. Vicksburg, MS: U.S. Army Engineer Research and Development Center.

Figure 1. Site location map of the Old River Control Complex (ORCC) (modified from Heath et al. 2015).

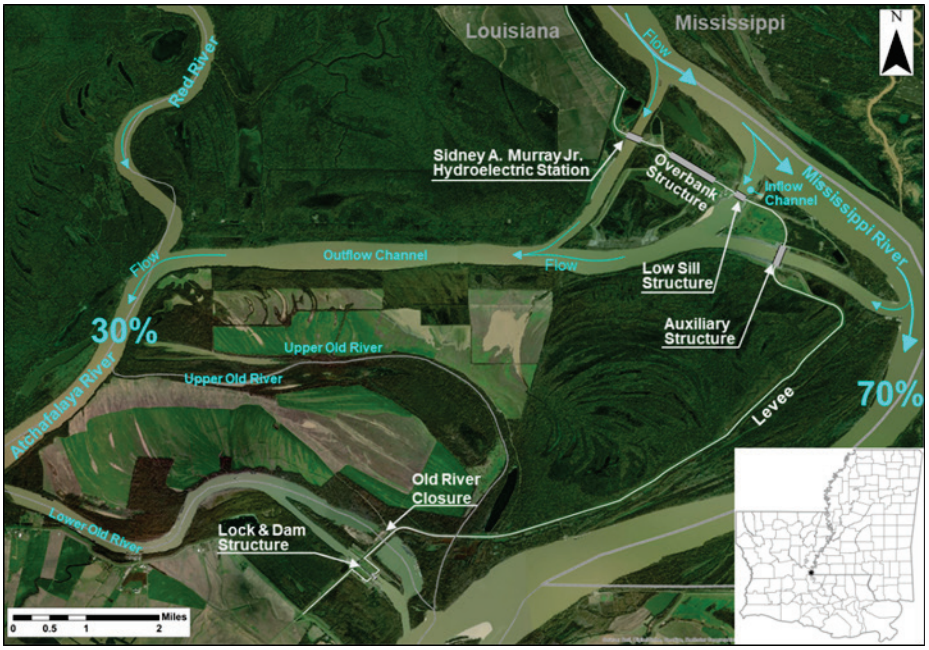

2 Geologic Setting

A detailed summary of geologic studies conducted at ORCC is provided by Breland et al. (2021*). The study area is located along the east-central border of Louisiana (Figure 1). The geology of the ORCC area consists of four depositional environments common to the Lower Mississippi River Valley, i.e., backswamp, natural levee, point bar, and abandoned channel deposits, as identified by Fisk (1947) and Saucier (1969, 1994).

Backswamp deposits are typically broad, topographically flat, clay-rich features that are deposited during high-water events where fine-grained sediments settle out of suspension. Natural levee deposits are wedge-shaped features adjacent to rivers along their banks. Natural levees are generally composed of relatively silty materials deposited when a river overtops its banks with relatively coarse-grained sediment depositing along the banks, which generally fines with distance from the riverbanks with a subsequent decrease in thickness. Point bars are deposited in an upward sequence of coarse- to fine-grained sands into silts and clays along the convex of a river as it migrates laterally. Arcuate ridges of sand separated by finer-grained clays and silts in swales develop parallel to subparallel to the river and are discerned by alternating topography. An abandoned channel deposit occurs when a river changes course, either gradually or instantaneously, followed by infilling of clay-rich sediment after a flood event. Eventually, an arcuate, topographically low, clay-rich deposit, also known as a clay plug, with a width comparable to the parent river remains. These geologic depositional environments dictate both soil and foundation conditions at the site.

2.1 Depositional environments

An assessment of depositional environments at Low Sill was provided by Breland et al. (2021*). Figure 2 (from Breland et al. 2021) shows a digital elevation model (DEM) with depositional environments, as previously discussed, and ORCC structures identified. The earthen levee centerline is indicated by the solid black line. Point bar deposits are discerned by the arcuate lines of alternating color in the image. The rill-shaped features are

*Breland, B. R., L. A. Walshire, J. R. Kelley, D. W. Harrelson, M. K. Corcoran, M. Zakikhani, J. E. Simms. 2021. *Old River Control Complex (ORCC) Low Sill: A literature synthesis.* Draft. Vicksburg, MS: U.S. Army Engineer Research and Development Center.

natural levee deposits with the higher elevations adjacent to the river that slope landward and, as described previously, decrease in thickness landward. The backswamp deposits are noted at the top left of the figure by the flat, broad, low-lying areas west of Overbank Structure. An abandoned channel is identified by the low-lying topography bounded by arcuate features.

2.2 Cross-sectional analysis

Borings from USACE (1954) were used by Breland et al. (2021*) to produce two lithologic cross sections based on the Unified Soil Classification System (USCS). One of those cross sections is replicated here (parallel to Low Sill, Figure 3). Cross section A-A' (Figure 3) was drawn northwest to southeast along the crest of Low Sill. From northwest to southeast, substratum sands (SP) are encountered at an elevation of -35.0 ft and overlaid by alternating silt (ML) and silty sand (SM) layers. A poorly graded sand (SP) layer, approximately 10.0 ft thick, is interbedded with ML and SM material at N-11. From N-13 to the southeastern end of the section are alternating layers of SM and ML with occasional CL clays and SP strata. Poorly graded gravel (GP) strata lie at an approximate depth of -65.0 ft and -100.0 ft Mean Sea Level (MSL) near Low Sill between borings N-13 and N-16. The GP unit was not encountered at N-17 in the inflow channel and N-15 in the outflow channel (Breland et al. 2021); however, boring penetration depths were less for N-17 and N-15 than the borings closest to Low Sill on cross section A-A'. A 10.0-ft-thick CH (fat clay) layer was encountered at a depth of -60.0 ft that extends laterally under the central portion of Low Sill and gradually thins eastward in the inflow channel. The top of substratum SP sands dips downward to a depth of -60.0 to -65.0 going southeast. The top of the Tertiary clays (CH) is shown in boring N-13 at a depth of -120.0 ft below MSL. The area between boring N-16 and the southern end of the section is the approximate profile of the grouted scour area.

*Breland, B. R., L. A. Walshire, J. R. Kelley, D. W. Harrelson, M. K. Corcoran, M. Zakikhani, J. E. Simms. 2021. *Old River Control Complex (ORCC) Low Sill: A literature synthesis.* Draft. Vicksburg, MS: U.S. Army Engineer Research and Development Center.

Figure 2. Depositional structures at ORCC, as indicated on the DEM map (Breland et al. 2021*).

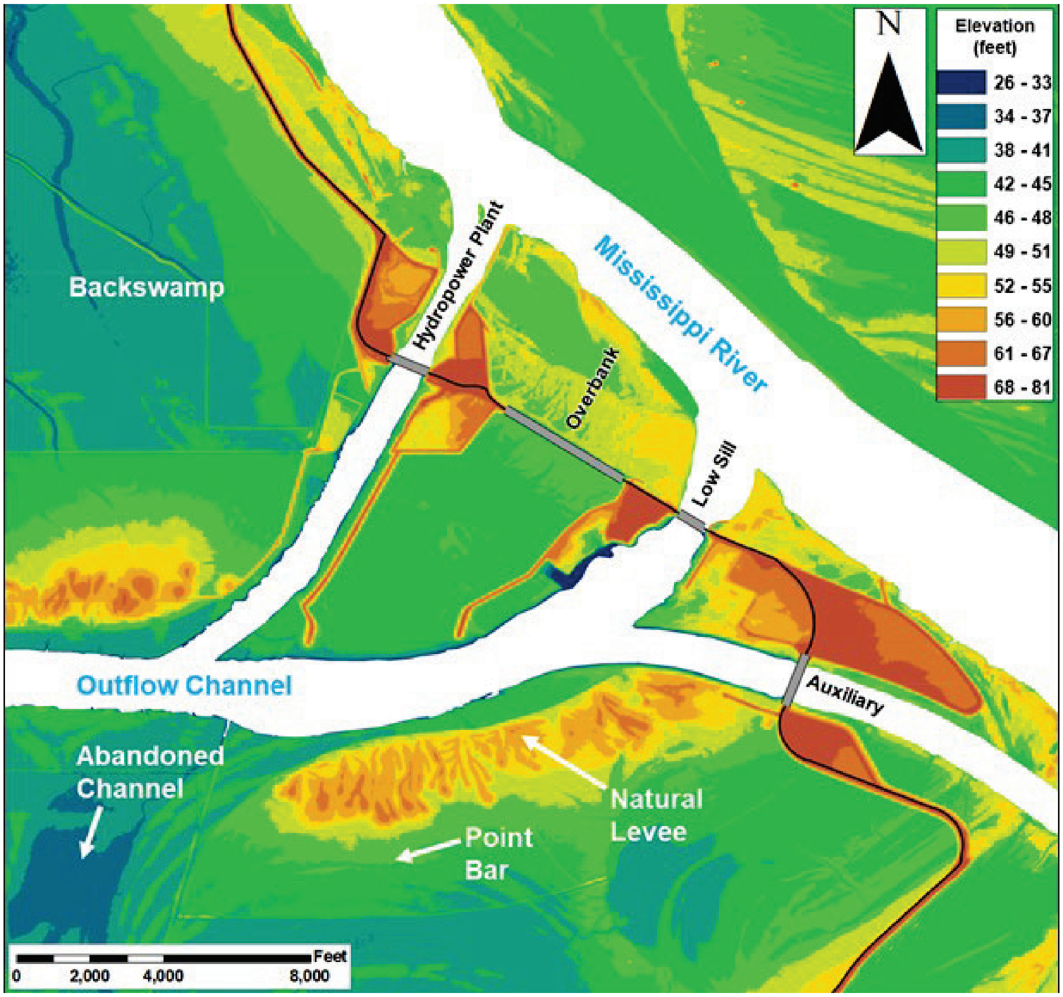

* Breland, B. R., L. A. Walshire, J. R. Kelley, D. W. Harrelson, M. K. Corcoran, M. Zakikhani, J. E. Simms. 2021. *Old River Control Complex (ORCC) Low Sill: A literature synthesis.* Draft. Vicksburg, MS: U.S. Army Engineer Research and Development Center.

Figure 3. Cross section A-A' across Low Sill (Breland et al. 2021*).

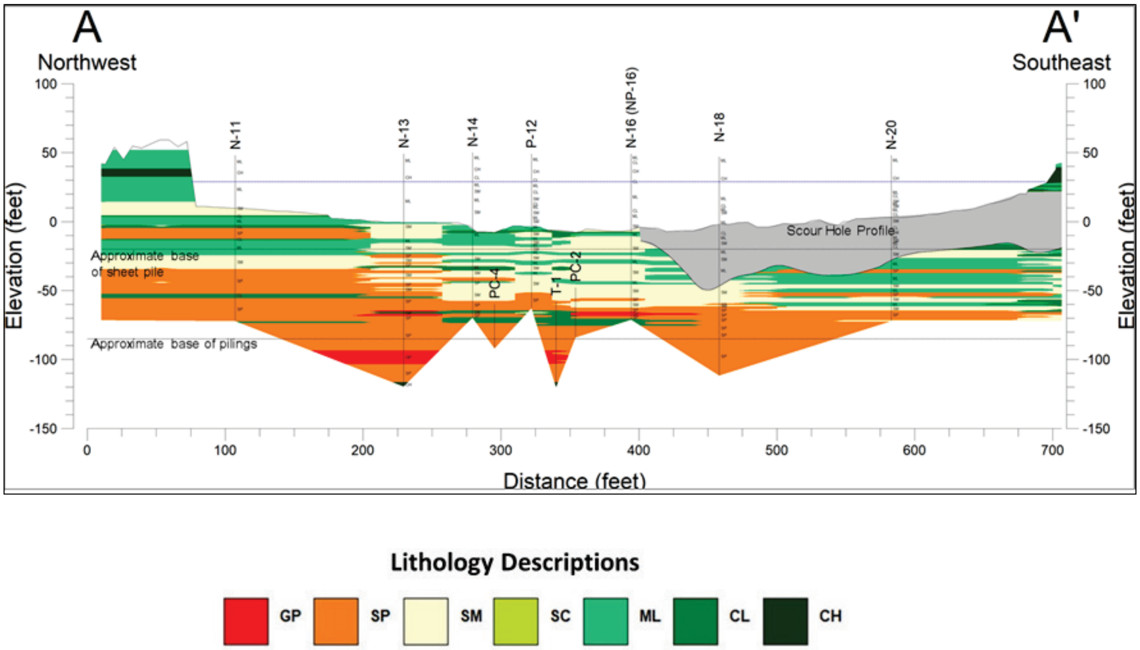

2.3 River elevation and water table

Depth to the water table at the study site is influenced by river stage because of the hydraulic connection between the Mississippi River Valley Alluvial Aquifer (MRVA) and the Mississippi River. River gauge elevations measured at the Low Sill inflow channel near Knox Landing are shown in Figure 4. River elevations were 8.6-9.0 m (28.5-29.5 ft) above MSL during the water-borne survey collection. Based on bathymetry surveys in the inflow channel, the approximate water depth was 7.0 to 10.6 m (23.0 to 35.0 ft) during the water-borne survey. River elevations were higher at the time of the land survey collection at 14.1-14.8 m (46.2-48.5 ft) above MSL. River elevations have typically been lower at this location in the past (from 1988 to 2017) with an average of 7.6 m (25 ft) above MSL.

Based on piezometer readings at Low Sill, the approximate water table elevation was 8.5-9.7 m (28.0-32.0 ft) above MSL or 4.0-7.6 m (13.0-25.0 ft) in depth from the land surface at the south side. Water table depths on the north side were approximately 10.9-12.2 m (36.0-40.0 ft) above MSL or 2.7-4.9 m (9.0-16.0 ft) deep. A nearby groundwater well site (USGS

* Breland, B. R., L. A. Walshire, J. R. Kelley, D. W. Harrelson, M. K. Corcoran, M. Zakikhani, J. E. Simms. 2021. *Old River Control Complex (ORCC) Low Sill: A literature synthesis.* Draft. Vicksburg, MS: U.S. Army Engineer Research and Development Center.

310638091381401), completed in the MRVA, lies 5.5 km (3.4 mi) northwest of the study area. Provisional readings of the water level show a depth of 2.0 m (6.45 ft) from the ground surface, or 11.7 m (38.5 ft) in elevation above MSL. The piezometer readings at Low Sill and the USGS well show a consistent depth to the water table during the land surveys.

Figure 4. Graph showing river elevation, in feet, in relation to time of geophysical survey collections.

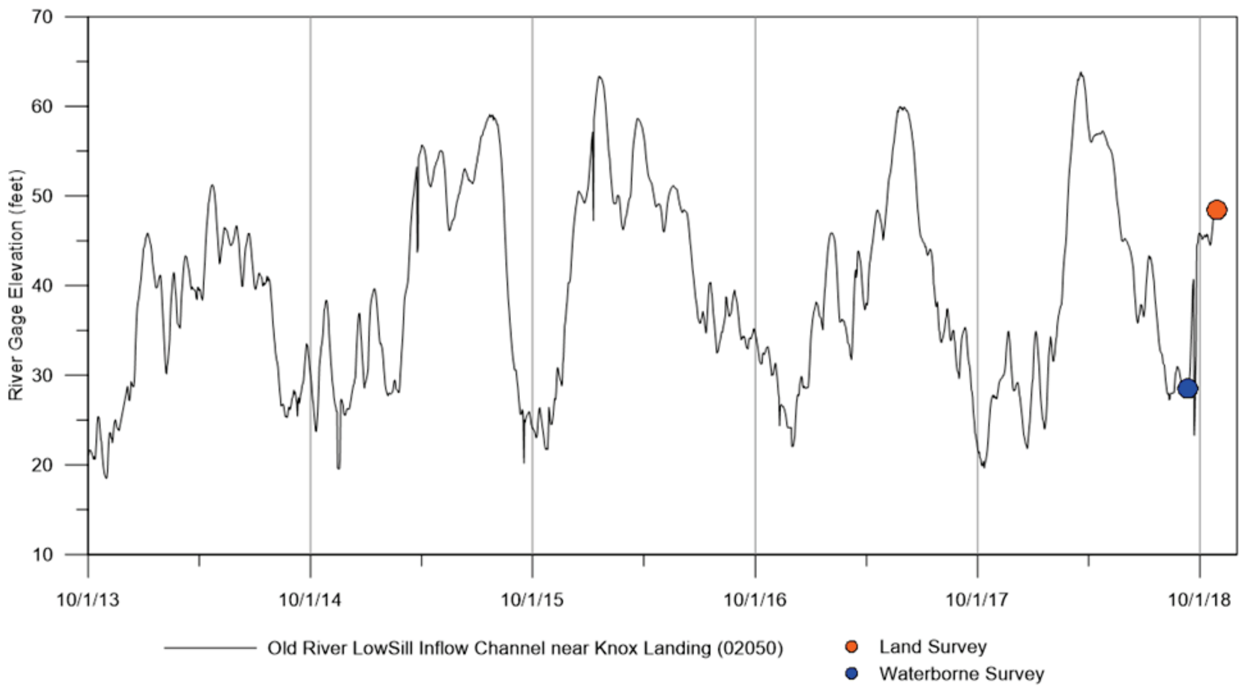

3 Site Description

Figure 5 shows map views of locations for the three resistivity lines and four seismic lines at Low Sill. Seismic lines are highlighted in red, and the resistivity lines are shown in white. Traffic along Highway 15, adjacent to both survey areas (north and south), caused short pauses in seismic acquisition because of the seismic noise generated by large vehicles, but this was not a significant problem. Similarly, small delays in seismic data acquisition were forced when large barges were in the channel, but these were sufficiently infrequent that their overall effect was minimal. For the north survey area, there were no known utilities crossed by the geophysical lines. An unpaved access road is located east of line LSNPL, and Highway 15 is located about 100.0-200.0 m south of all lines in the north survey area. During seismic data acquisition, heavy equipment was operating at USACE facilities a few hundred meters south of Highway 15 and served as a significant noise source that required many pauses in data acquisition for line LSNPD. Heavy rains overnight on October 31 forced a hiatus in heavy equipment work, and this provided unimpeded seismic acquisition November 1-2. In the south survey area, there were power lines alongside both the seismic and resistivity lines for about 100.0 m. In some cases, such lines can cause strong 60-Hz interference in both data sets, but there was no noticeable power line interference in either data set.

At the time of the water-borne GPR survey, the Old River Channel was considered to be at low water level, and all 11 gates were closed.

Figure 5. Location of resistivity and seismic lines. (a) Line locations on the northeast side of Low Sill, and (b) line locations on the southeast side.

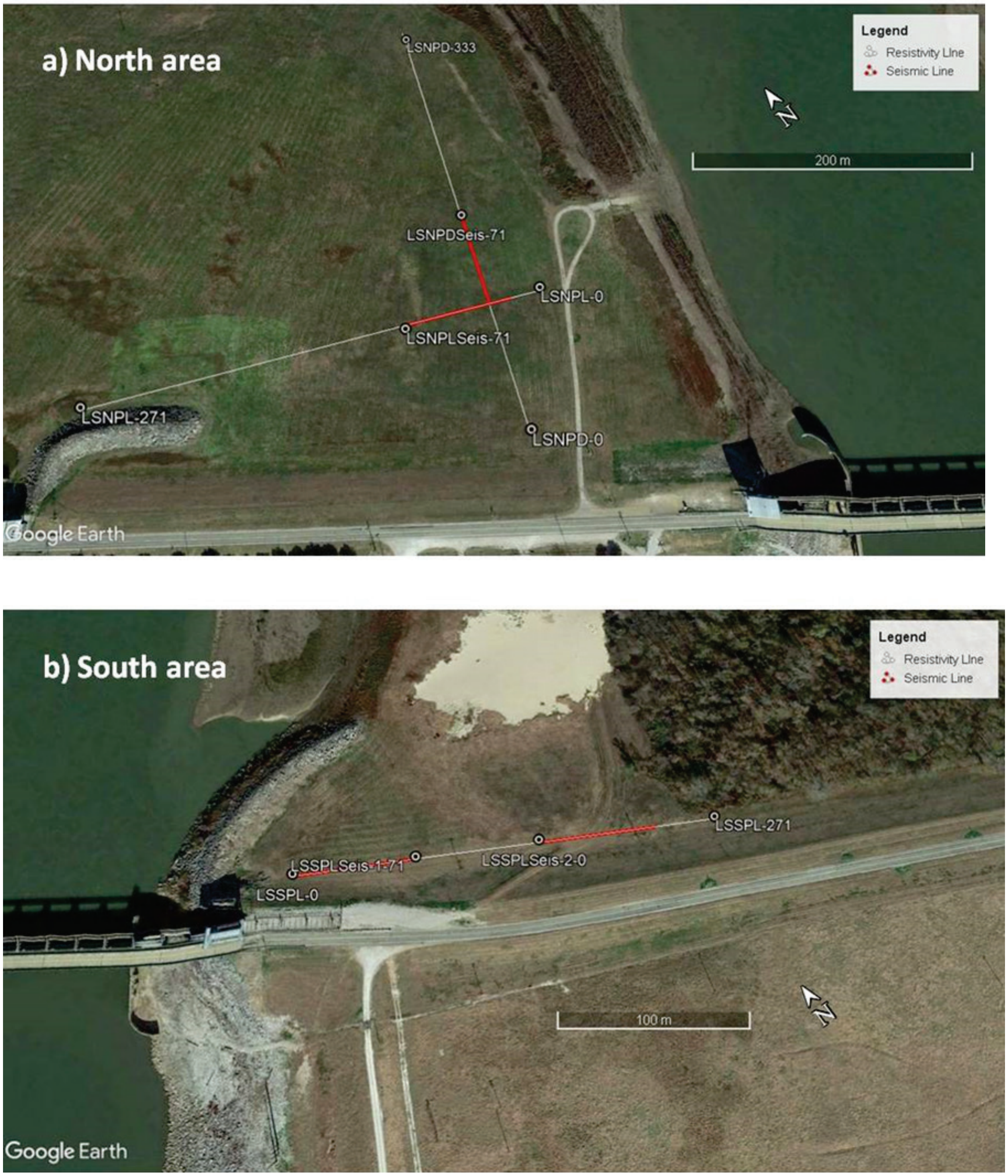

4 Data Acquisition and Processing

Electrical resistivity tomography (ERT) data and seismic refraction tomography (SRT) data were acquired on land on both sides of the Low Sill structure during the week of 29 October 2018. Data were acquired on two orthogonal ERT lines on the northeast side of the structure; ERT Line LSNPL, aligned parallel to the structure, had a length of 249.0 m, and ERT Line LSNPD, perpendicular to the structure, had a length of 333.0 m (Figure 5a). On the southeast side of the structure, ERT Line LSSPL had a length of 249.0 m (Figure 5b). Because of dense vegetation (not seen in Figure 5b because of a lapse in mowing when the satellite photo was acquired), it was not possible to acquire a perpendicular ERT line on the south side of the structure. All ERT lines had an electrode spacing of 3.0 m and used 84-electrode cables.

The SRT lines were all 71.0 m in length (1.0-m geophone spacing with 72 channels). This length was constrained by the distance from the seismic sledgehammer energy source to which signal could be reliably detected. Longer lines would have required a more powerful energy source, which was not available at the time of the deployment. On the northeast side of the structure, SRT Line LSNPD was acquired over a portion of ERT Line LSNPD, and SRT Line LSNPL was acquired over a portion of ERT Line LSNPL. Two SRT lines were acquired along separate segments of the southeast-side ERT Line LSSPL, named Lines LSSPL-1 and LSSPL-2.

4.1 Electrical resistivity

An electrical resistivity survey measures how well an electrical current flows through the subsurface. Resistivity is the inverse of conductivity, i.e., low resistivity translates to high conductivity. A single measurement involves four electrodes, two current and two potential electrodes generally positioned along the same line, connected by wire to the resistivity instrument. An electrical current is introduced into the ground through one current electrode and flows to the other, and the potential difference between the two potential electrodes is measured. Knowing the amount of injected current and the measured potential, the resistance can be calculated. Resistivity (unit ohm-m) is a property of the volume interrogated and can be determined by multiplying the resistance by a geometry factor, which is related to the arrangement of the four electrodes. The four-electrode arrangement is called an array, and there are different array types depending on the survey objective. For this survey, a dipole-dipole array was used. This array uses four electrodes linearly arranged to acquire a single measurement, with the two current electrodes (left side) and two potential electrodes (right side) equally spaced, a, but separated by a multiple, na, of the current (or potential) electrode spacing (Figure 6a). At large n (about 8), the potential difference generally becomes too small to measure so both the current and potential electrode pairs are shifted one electrode and the process repeated. By increasing the spacing between both current and potential electrode pairs and/or the two current (potential) electrodes, both lateral and vertical information about the subsurface are obtained. In this manner, it is possible to obtain a 2-D image of the subsurface. Because of the nature of measurements using an increasing electrode spacing, the number of measurements at depth decreases as the electrode spacing increases. Thus, the subsurface area imaged is similar to that of an inverted triangle. The dots in Figure 6b represent pseudo-depth locations of resistivity measurements for given electrode spacings. Modern ER systems allow initial placement of electrodes and electrode cables and use automatic switching capabilities to measure multiple electrode combinations.

An Advanced Geosciences Inc. (AGI) SuperSting™ R8 earth resistivity system with an electrode switch box was used to acquire the resistivity data. It consists of a control unit and electrode switch box, powered by a 12-volt deep-cycle marine battery (Figure 7). This is an eight-channel system, meaning eight readings, i.e., electrode pairs, are acquired during one measurement. A layout of 112 electrodes was used with eight cables of 14 electrode take-outs. The electrode spacing was 3.0 m with a maximum na spacing of 24.0 m, giving a total line length of 333.0 m. The electrodes were approximately 46.0-cm (18.0-in.) length steel rods hammered about 15 cm deep.

Data were processed using the AGI EarthImager 2-D resistivity inversion software. The processing sequence included removal of noisy data, defining the forward model method and type of boundary conditions, and setting the inversion parameters. The inversion technique uses a damped least-squares approach. The inversion output is a 2-D color plot of resistivity with depth. The “hot” colors (red) represent higher resistivity values, whereas the “cold” colors (blues) represent lower resistivity values. In the data plots that follow, the color bars are not plotted on the same scale; therefore, it is important to observe the magnitudes on the scale bar rather than looking at just the high and low colors. All color bars will have a blue (low) to red (high) scale regardless of the range of resistivity values.

Figure 6. (a) Dipole-dipole electrical resistivity configuration. By using different values for a and n, 2-D coverage of the subsurface is obtained (b). In (b), the rectangles along the surface represent electrodes (in this example 56), and the dots in the subsurface represent the pseudo location of a measurement. For a given number of electrodes, as the electrode spacing increases, the number of measurements at depth decreases.

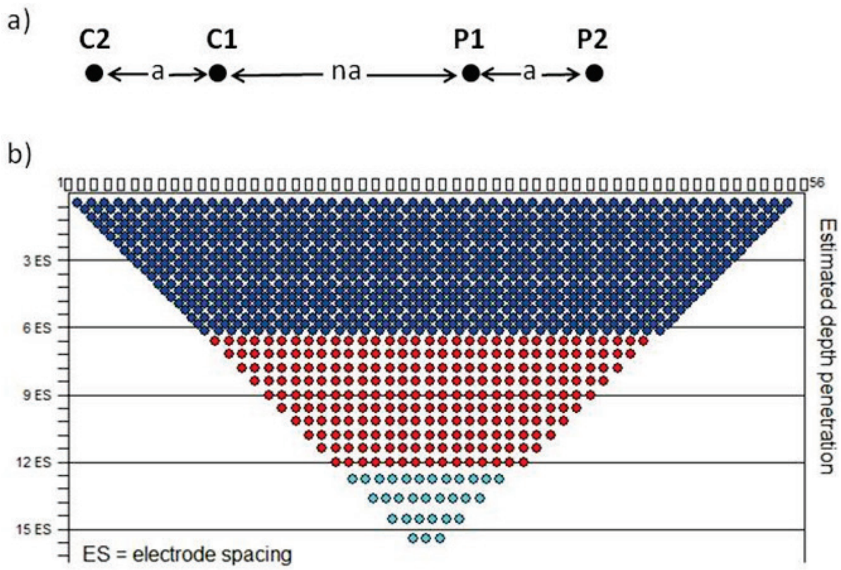

Figure 7. Advanced GeoSciences Inc. SuperSting™ R8 system used to acquire the electrical resistivity data.

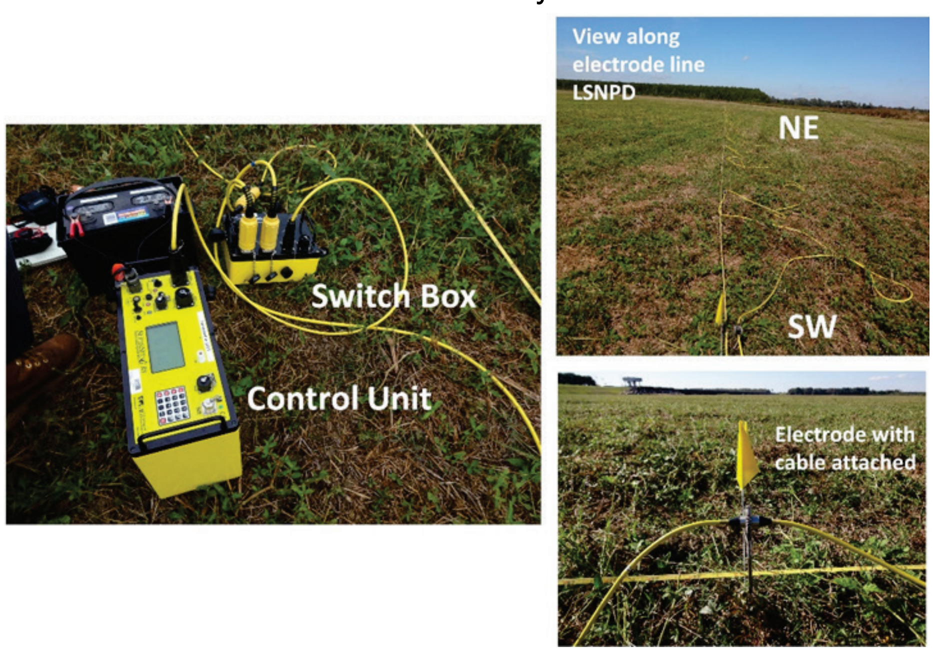

4.2 Seismic refraction tomography

There are several seismic methods that can be used for shallow site characterization, from which a selection is made based on the problem of interest, depth range, and geologic properties of the site. Seismic refraction methods involve analysis of the travel times from a seismic energy source to each sensor (geophone) in a linear array. Collection of seismic measurements at a series of source locations within and off the ends of the geophone array enables a cross-sectional image of seismic velocities to be produced for a vertical plane beneath the geophone array. The first step in seismic refraction analysis is to measure the travel times for every source "shot point" and every sensor position for those shot points (Figure 8). Generally, seismic refraction acquisition and processing are designed to determine the seismic P-wave velocities, but these surveys can also be designed to determine S-wave velocities. After measuring the travel times, a suite of analysis methods is available, ranging from methods that determine layered model solutions to "tomographic" solutions that allow more lateral variation in the seismic velocities. These velocities are characteristic of certain rocks or soils and vary depending on the distribution of rock and soil units in the subsurface. When seismic and resistivity cross sections are compared, changes in either rock or soil types can often be determined with greater confidence.

Seismic data were acquired with a 72-channel Geometrics Geode system using an 18-lb sledgehammer as the seismic energy source and 4.5-Hz geophones as receivers at 1.0-m spacing (Figure 9). The sledgehammer shots were typically located at 12.0 m and 24.0 m off the ends of each line, and at 3.0-m intervals within each line. Four to eight hammer blows were combined at each shot point to improve signal strength.

Figure 8. Travel times of first-arriving seismic waves, indicated by “x” in the top portion of the figure, can be compiled for all shot points, as shown in the bottom portion of the figure. These travel times are compared to travel times from models that are iteratively adjusted to improve the fit of the model to the data, in a process known as inversion.

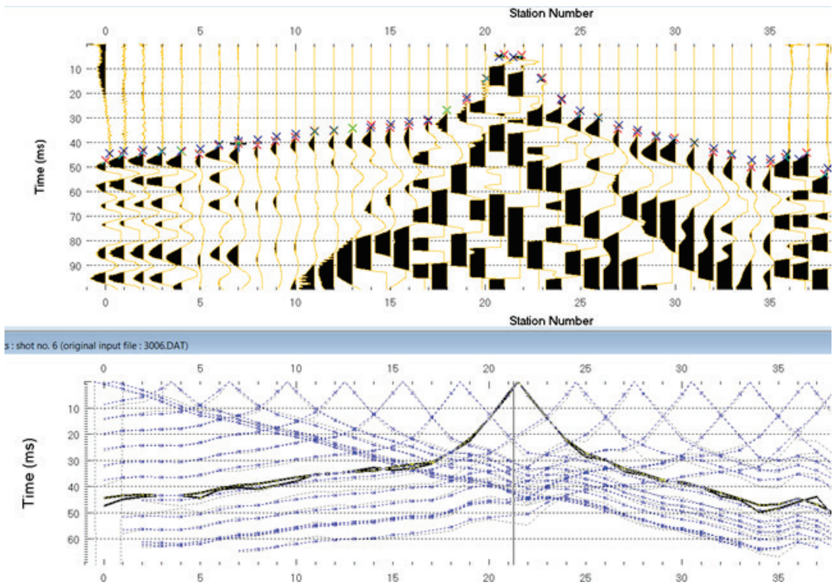

Figure 9. Seismic data acquisition components.

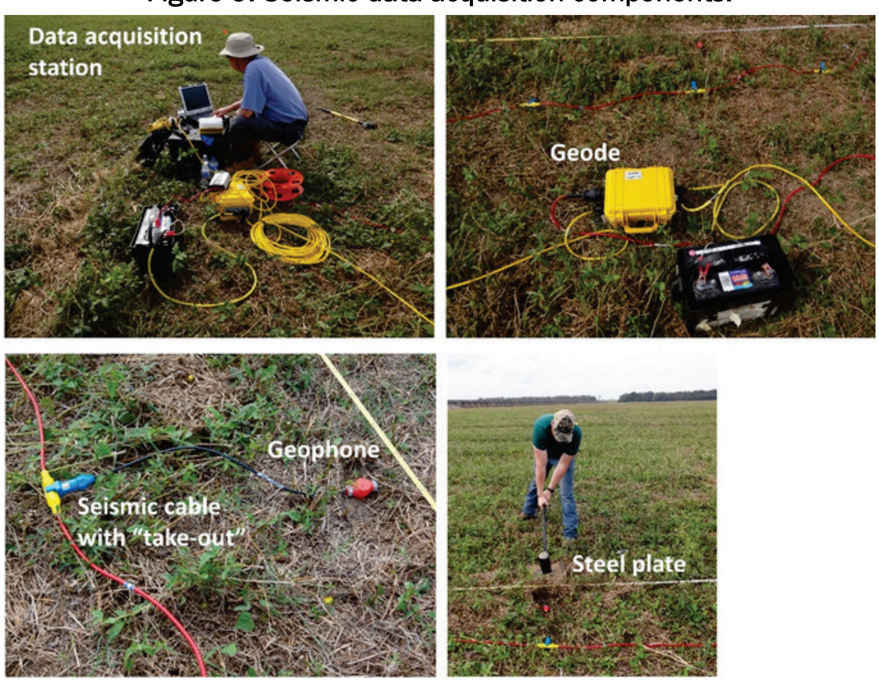

4.3 Ground penetrating radar (GPR)

The GPR data were acquired using a GSSI Model 3200 MLF Multiple (Adjustable) Low-Frequency Antenna with a SIR4000 control unit. The system has adjustable transmission frequencies ranging from 80 MHz to 16 MHz, allowing deep penetration of the subsurface. The system was adapted to a water-borne survey by mounting it on inner tubes and using polyvinyl chloride (PVC) pipe to maintain a fixed separation between the transmitter (Tx) and receiver (Rx) antennas for a given antenna frequency (Figure 10). A Trimble GeoXH 6000 GPS was linked to the GPR system to provide positioning information. It was positioned in an inner tube midway between the ends of the transmitter antenna. The GPR system was towed behind a boat in a back-and-forth pattern across the width of the inflow channel. Data were viewed and stored on the SIR4000 during collection and later imported into the GSSI RADAN software for processing.

The electrical conductivity of the water is an important factor for a successful water-borne GPR survey. A YSI 600R Water Quality Sonde was used to measure the water conductivity and temperature between the surface and 25.0-ft depth at 5.0-ft intervals (Figure 11). It is necessary to acquire temperature data because electrical conductivity varies with temperature, and the readings must be corrected. Prior to any measurement, the sonde was initially calibrated using a standard 12,880 µS/m solution.

Figure 10. GSSI Model 3200 MLF with 35-MHz antenna and Trimble GeoXH GPS.

Figure 11. YSI 600R Water Quality Sonde used to measure electrical conductivity and temperature of the water.

5 Results

5.1 Electrical resistivity

Three land-based electrical resistivity profiles were acquired, i.e., two on the northeast side of the Low Sill structure and one south of it (Figure 5).

5.1.1 North area

Electrical resistivity inversion cross sections of the northeast survey area are given in Figure 12. For both lines, data indicate a layered sequence with variable layer thicknesses and lateral discontinuities, either associated with pinch-outs of a stratigraphic feature or compositional changes within a layer. Higher resistivity values are associated with sandy or silty units, and lower resistivities indicate higher clay content. There is a recognizable lateral change in the shallow structure (depths 0.0-20.0 m) that occurs around x=189.0 m on line LSNPL. Also, the deeper clayey layer (depth ~15.0 m) is more continuous on line LSNPD. The deeper high resistivity layer at 25.0- to 45.0-m depth is largely unaffected by this lateral change. There is good agreement between the two cross sections at their crossing point, indicated by the vertical dashed line on both profiles.

5.1.2 South area

Electrical resistivity inversion results for line LSSPL in the southeast area are presented in Figure 13. This section indicates a layered structure in the western portion of the line but a much more complicated structure in the eastern portion between x=168.0 m (634090.94E, 3438794.56N) and x=210.0 m (634128.25E, 3438775.44N). The layered structure in the western portion is significantly different than that in the northeast area, with a more prominent sandy layer in the upper 5.0 m, thicker clay layer between 5.0-15.0 m, siltier layer 15.0-28.0 m, and the presence of clay deeper. Data from this line are plotted on the same color scale as was used in the northeast area. It is noteworthy that both the high and low resistivity values here are more extreme than they were in the northeast area.

Figure 12. Inversion results for the northeast resistivity survey lines, LSNPD and LSNPL. The dashed vertical line on both cross sections marks where the two lines cross.

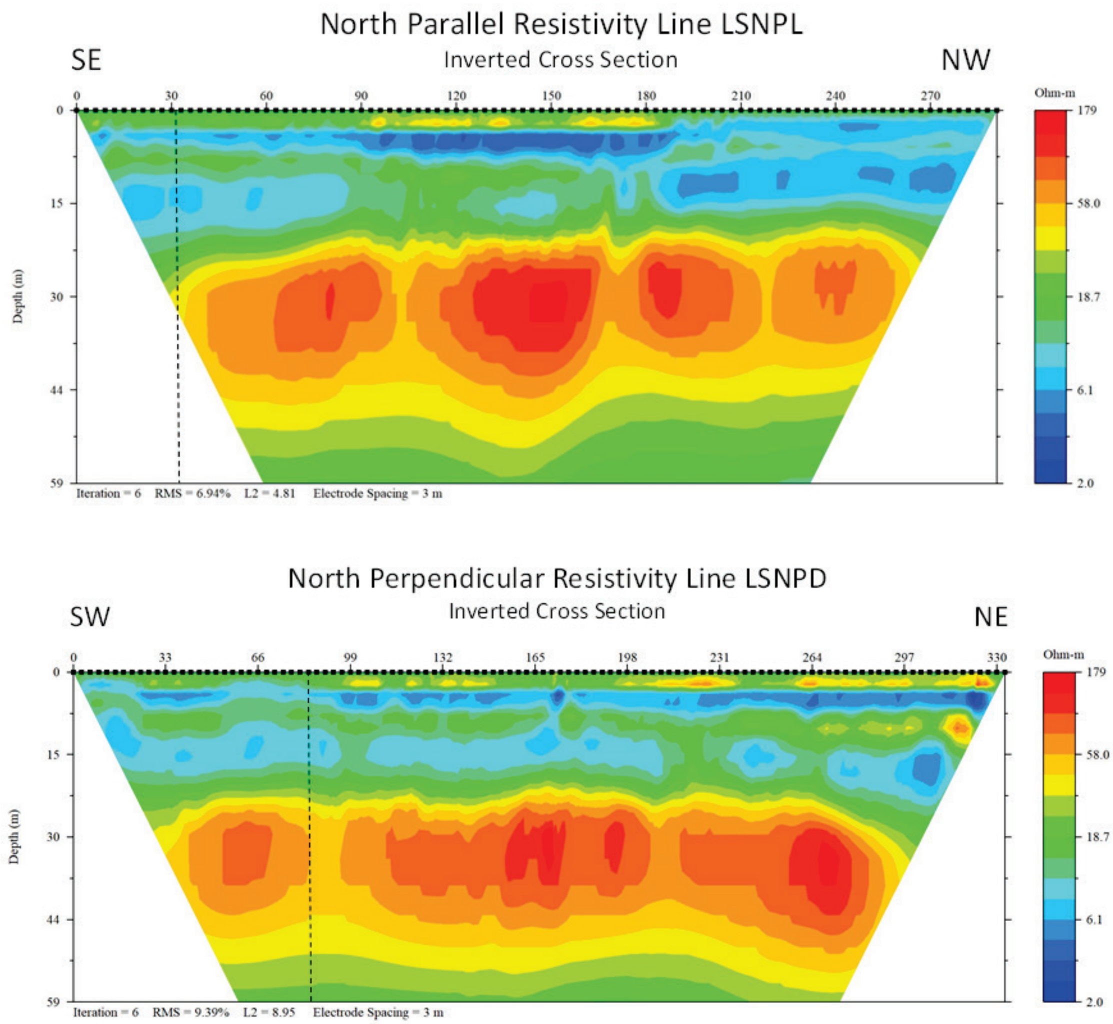

Figure 13. Inversion results for the southeast resistivity survey line, LSSPL.

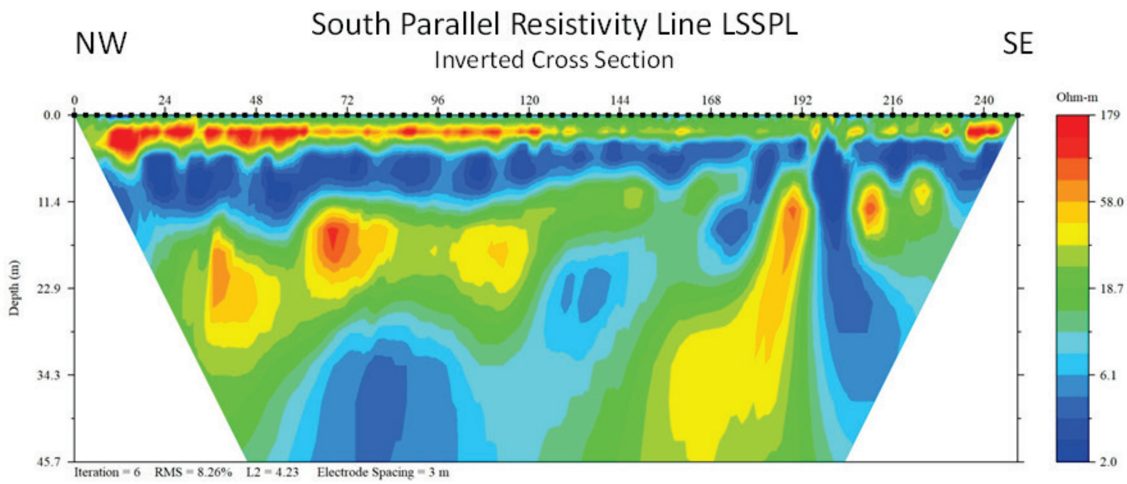

5.2 Seismic refraction

The processing of the seismic refraction data was complicated because the site response did not follow the usual behavior where velocities increase with increasing depth. On line LSSPL-2 in particular, a low-velocity zone is indicated at about 6.0- to 12.0-m depth and similar, but less extreme, low velocity features are observed on the other lines. Some of the low-velocity features might be indicative of sand or similar low-velocity material, with the surrounding higher velocity features associated with clays or more compacted clastic sediments. Conventional seismic refraction methods that are designed for layered structures are known to be incapable of properly imaging low-velocity layers. Tomographic processing methods are able to detect such features, although they might assign improper velocities to them and might mis-identify shapes and sizes of such features. Processing and interpretation of seismic data in such situations must proceed with care and awareness of the uncertainties and pitfalls that can be encountered and of the non-uniqueness of tomographic solutions, particularly in the presence of low velocity zones.

The Rayfract software package offers several options for handling seismic refraction data as indicated earlier. For the LSCS data set, after a series of trials and consultation with the software provider, a Delta t-V method was used to create the starting model, followed by an iterative Waveform Eikonal Tomography (WET) approach to produce the final cross sections. Processing parameters were selected to allow reasonable model depths and smoothing to emphasize features of interest without including a level of detail that is unwarranted. The processed seismic refraction cross sections are provided in Figures 14 (northeast side) and 15 (southeast side).

Figure 14. Processed seismic results for northeast side lines LSNPL (top) and LSNPD (bottom).

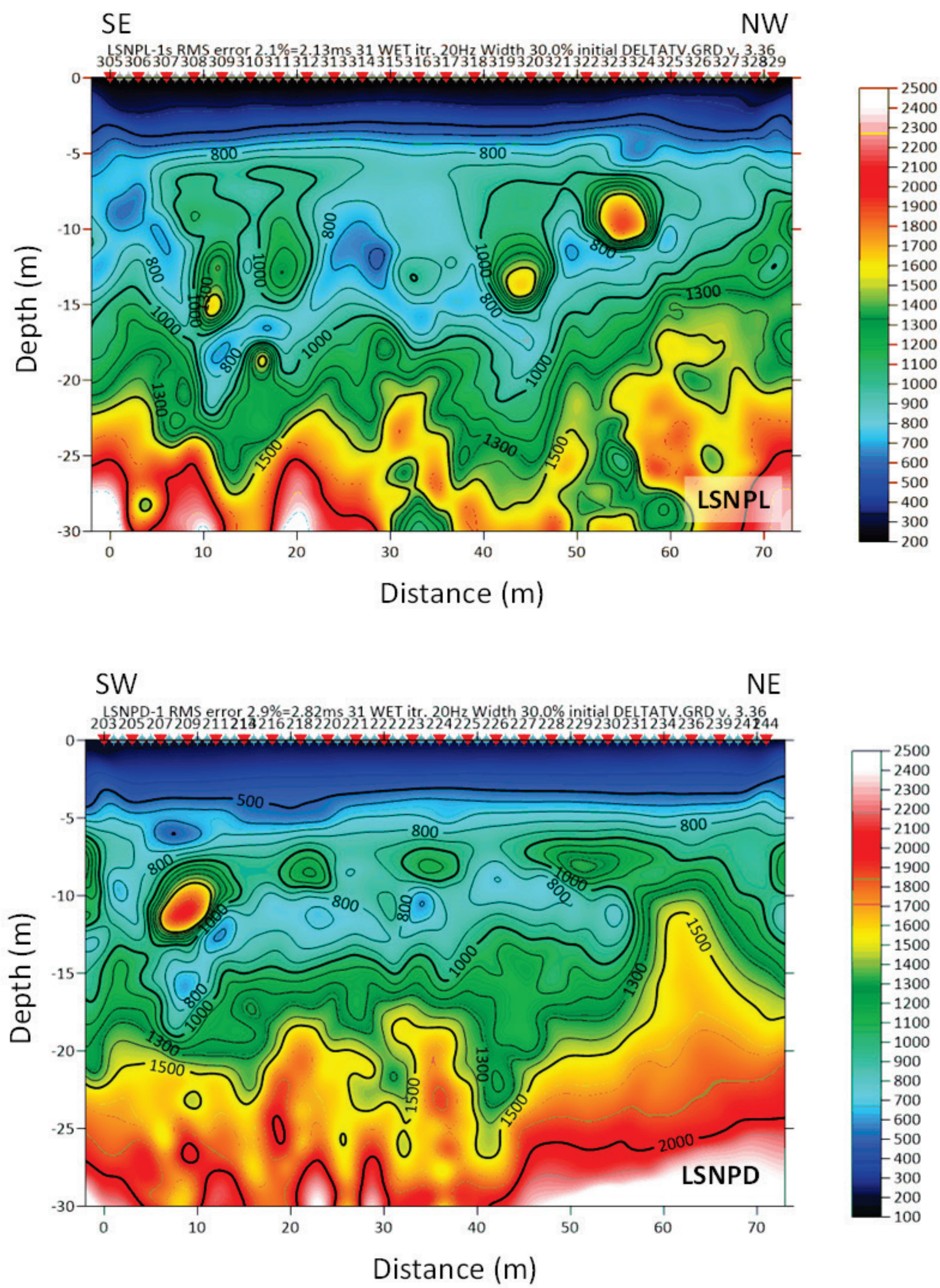

Figure 15. Processed seismic results for southeast side lines LSSPL-1 (top) and LSSPL-2 (bottom).

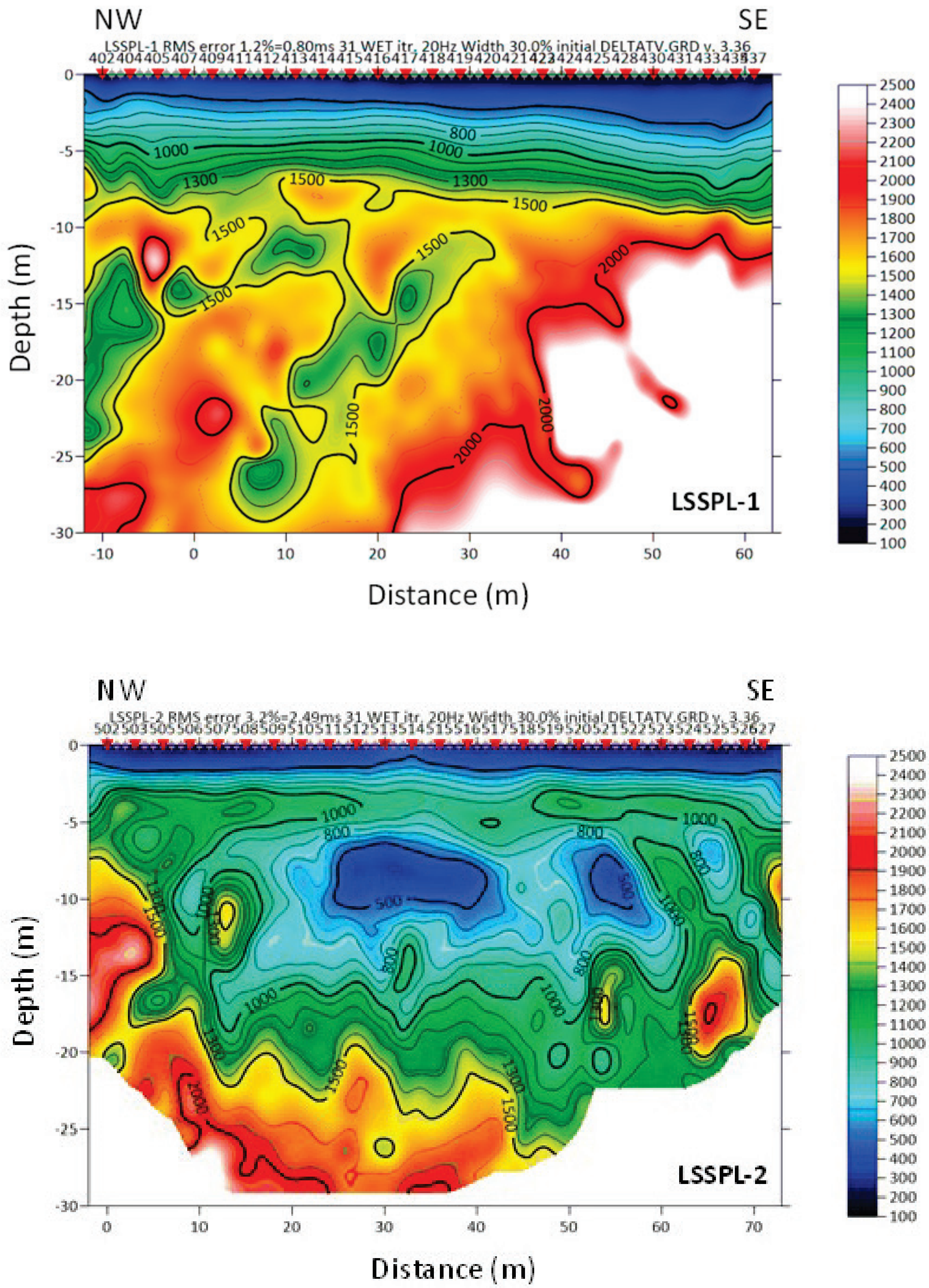

5.2.1 North area

On the northeast side of LSCS, seismic lines LSNPL and LSNPD show a slightly undulating layered structure between the surface and a depth of 5.0 to 6.0 m, with velocities mostly less than 800 m/s (Figure 14). Beneath that is a zone with more lateral variability in velocities that extends to about 20.0-m depth with velocities varying between about 600 m/s and 1500 m/s. The depth of the 1500 m/s contour is variable but mostly between about 15.0-m and 25.0-m depth. This contour is usually indicative of the water table, but at this site it occurs at greater depth than the water table, which is estimated between 2.0 m to 5.0 m. This discrepancy is likely because of the high degree of lateral variability in seismic velocities and the presence of low velocity zones, which could cause the modeled velocities to be lower than actual values.

5.2.2 South area

The seismic lines on the southeast side of LSCS, LSSPL-1 and LSSPL-2, have significant differences from one another and from the lines on the northeast side. LSSPL-1 has a layered structure at the surface, similar to that on the northeast side, except that it extends to greater depth, dipping from about 7.0-m depth on the west (left, on top portion of Figure 15) to about 10.0-m depth at the east end of the line. The velocity at the base of this structure is 1500 m/s, whereas it was only about 800 m/s for the lines on the northeast side. Beneath this layered structure on LSSPL-1 there is some lateral variability in the velocities, although it is not as extreme as observed on the northeast side, and there is a general trend from lower velocities (about 1300 m/s) on the west end to more than 2000 m/s on the east end of the line.

In contrast, the thickness (about 2.5 m) of the shallow layered structure is less on line LSSPL-2 (bottom portion, Figure 15) than on either LSSPL-1 or the lines on the northeast side and reaches about 800 m/s at its base (similar to the velocity at the base of this unit on the northeast side). The layered structure might continue to about 6.0-m depth except that it is disrupted with lower velocities in the center of the line. Underneath and extending laterally from the disrupted portion of the shallow layered structure, there is a large low velocity zone, 5.0-10.0 m in height and 50.0 m or more in width with velocities less than 500 m/s. There are portions of this low velocity zone that have higher velocities, and it is flanked by higher velocities. On the west end of the line, velocities in excess of 1500 m/s are found as shallow as about 7.0 m.

5.3 Ground penetrating radar

The water-borne GPR survey did not result in a usable data set because of the high electrical conductivity of the water. The average measured conductivity was 52.0 mS/m. Much of the transmitted signal was absorbed by the water column with limited to no penetration into the sub-bottom sediments. An example of the data using the 40 MHz antenna is shown in Figure 16. The horizontal axis represents radar scan number and the vertical axis depth in feet. The line path was along the length of the structure in front of the monoliths. Note that the only reflections discernible in the profile are the air wave reflections off the LSCS monoliths. If signal penetration had been achieved, the bottom of the channel would appear at a minimum depth of 20.0 ft.

Figure 16. Example of water-borne GPR profile acquired with a 40-MHz antenna. The reflections seen in the upper part of the profile are caused by the air wave; one is received from each monolith. The white-dashed vertical lines are fiducial marks placed in the data while the data were being collected and correspond to the location of the antenna when it passed in front of a monolith.

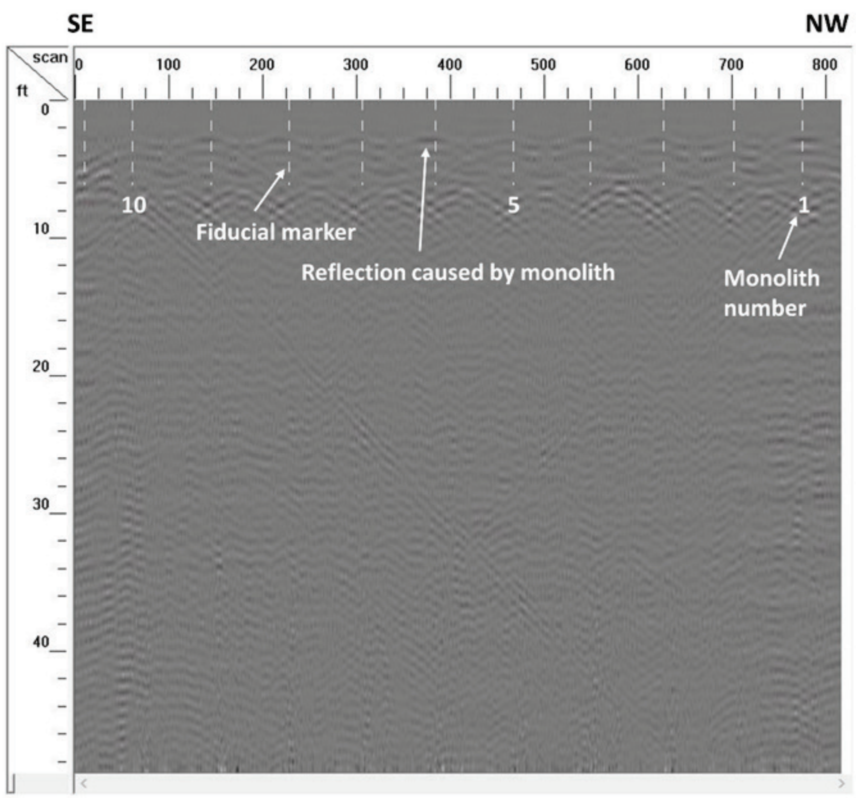

6 Interpretation and Joint Analysis

As a first level of interpretation, the resistivity results can be compared with the cross section derived from boring logs (Figure 3). To do this, the two parallel resistivity sections, LSNPL and LSSPL are scaled and superimposed adjacent to the cross section from Figure 3, as shown in Figure 17. Listed in Table 1 are typical relative geophysical properties of soft sediments, such as those encountered at LSCS. These do not address the influence of water, particularly below the water table, which tends to decrease electrical resistivity and increase seismic velocity, especially if the water contains salts or other electrolytes. These represent the end members among sediment types likely to be encountered at LSCS. Silts, or mixtures of silts with clays or sands, will tend to have intermediate values. Fat clays have lower resistivities than lean clays.

Figure 17a represents the relationship between resistivity and stratigraphy on the northeast side of ORCS. The lowest resistivities match a fat clay layer (CH) at 3.0-4.0 m depth in the resistivity section. Beneath that, at 4.0-11.0 m, is a silty sand layer with higher resistivities. At 11.0-17.0 m, a lean clay layer (with central thin sand layer at boring N-11, which may be absent over some or all of the area covered with the resistivity lines) has resistivities that are higher than the fat clay at 3.0-4.0 m but lower than the silty sand at 4.0-11.0 m. Beneath this is a silty sand layer with similar resistivity to the layer at 4.0-11.0 m, and at the base is a thick sand layer with the highest resistivity of the section.

Table 1. Relative geophysical properties of sands and clays.

Property	Clays	Sands
Electrical Resistivity	low	high
Seismic Velocity	high	low

Between the two geophysical study areas, the stratigraphy that is indicated from the boring logs changes radically between adjacent wells. This is an indication that a layer-cake structure is unlikely to be encountered as one moves across the dam into the southeast area. In addition, the scour area yields a cross section in which much of the original stratigraphic section is missing in Figure 3. As a result, it is not reasonable to correlate stratigraphic units on the southeast side in the manner that was possible on the northeast side; however, based on the correlation of sands and clays on the northeast side with high and low resistivities, it is reasonable to project possible soil types on the red and blue resistivity areas on Figure 17b.

To assist in interpreting the seismic refraction data, it is useful to overlay the contours from the seismic data on the resistivity sections, as shown in Figures 18-20. Selected features, to be discussed in the following paragraphs, are identified with lettering, where black letters indicate seismic velocities that are low relative to their surroundings and white letters represent relative high anomalies.

Figure 18 shows the seismic contours superimposed on the southeast portion of the resistivity section for northeast line LSNPL. Three high-velocity anomalies are identified as A1, A2, and A3. The 500-m/s velocity contour at about 4.0-m depth correlates well with the top of a low conductivity (blue) layer across the entire seismic profile. Beneath the low conductivity layer and corresponding to the 800-m/s seismic contour, seismic and resistivity sections do not show much correlation, presumably because they are responding to different attributes of the sediments, i.e., resistivity response is primarily influenced by the presence of water, whereas seismic response is influenced more by material type and density. Seismic anomalies A2 and A3 both lie in proximity to low resistivity peaks (darker blue), where the correspondence of higher velocities and lower resistivities might correspond to higher clay content, but anomaly A1 (the shallowest of the three "A" anomalies in Figure 18) does not appear to have a corresponding response in the resistivity.

Figure 19 shows the overlay of seismic contours on resistivity for the southwest end of northeast line LSNPD. As with LSNPL, the 500-m velocity contour corresponds well with the top of the low resistivity (likely clay) layer at 3.0- to 4.0-m depth. Likewise, the base of this low resistivity layer corresponds with seismic velocities of 800-900 m/s. As with anomaly A1 on line LSNPL, there are high velocity anomalies, here identified as B1, B2, B3, and B4, in the more resistive layer at 7.0- to 12.0-m depth; however, there are not high velocities in the underlying low resistivity layer at 12.0- to 17.0-m depth that would correspond to anomalies A2 and A3 on line LSNPL. There is a low velocity feature, identified as C1, on line LSNPD that is positioned in proximity with a gap in the low resistivity layer at 12.0- to 17.0-m depth.

Figure 17. Correlation of resistivity cross sections with stratigraphic cross sections: (a) northeast side (the resistivity cross-section segment is reversed relative to its orientation in Figure 12); (b) southeast side. The vertical scales are approximately the same, and vertical position is aligned.

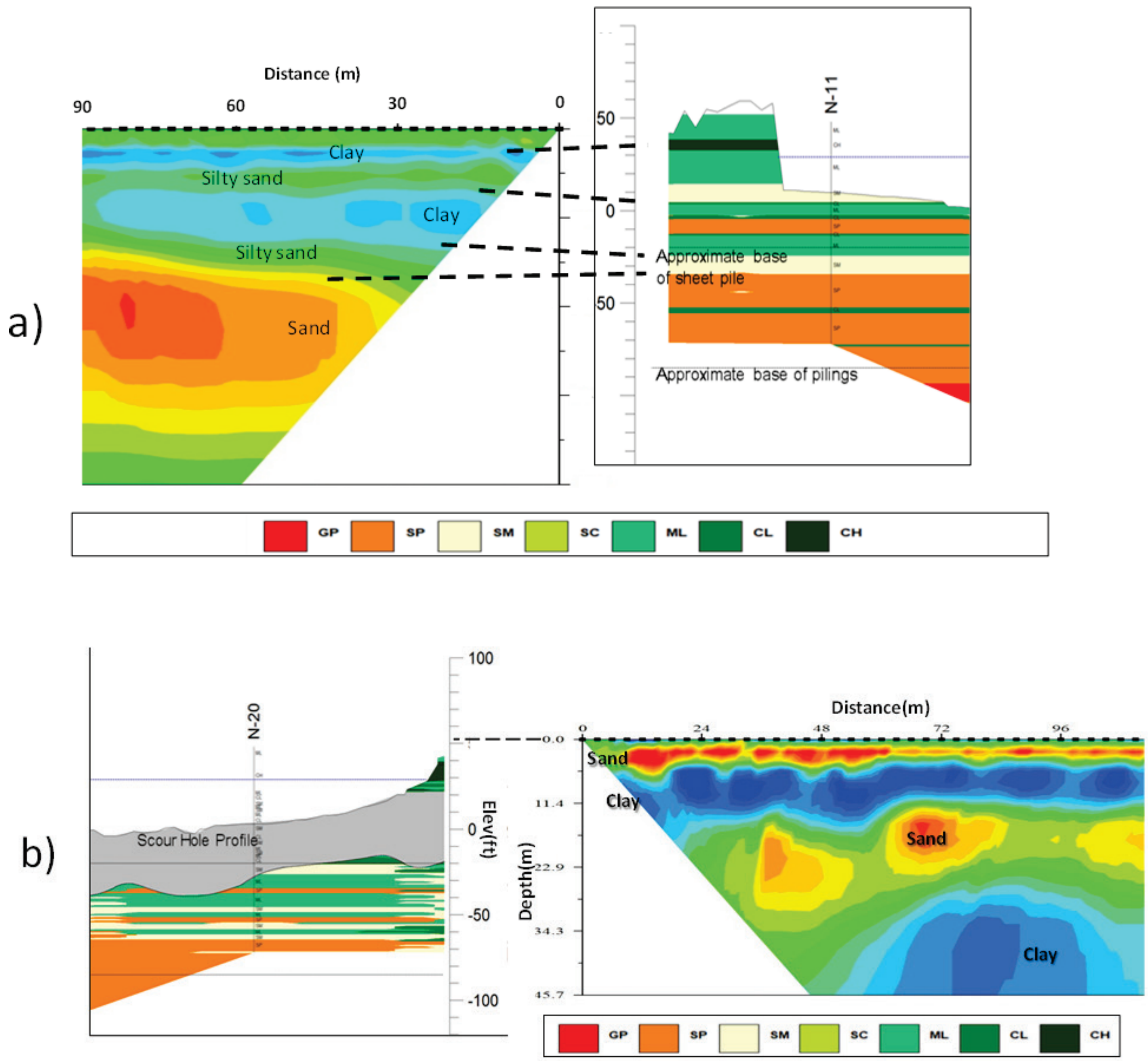

Figure 18. Overlays of seismic contours on resistivity section for northeast line LSNPL. White lettering is used to represent relatively high seismic anomalies.

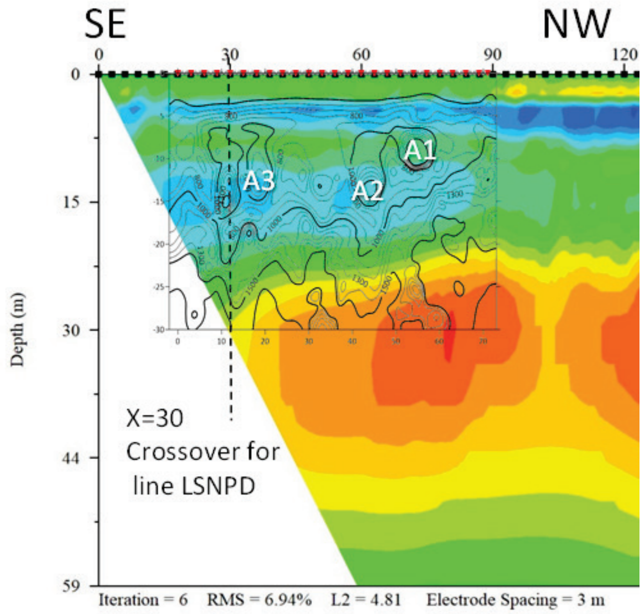

Figure 19. Overlay of seismic contours on resistivity section for northeast line LSNPD. White lettering is used to represent relatively high seismic anomalies; black lettering represents relative low anomalies.

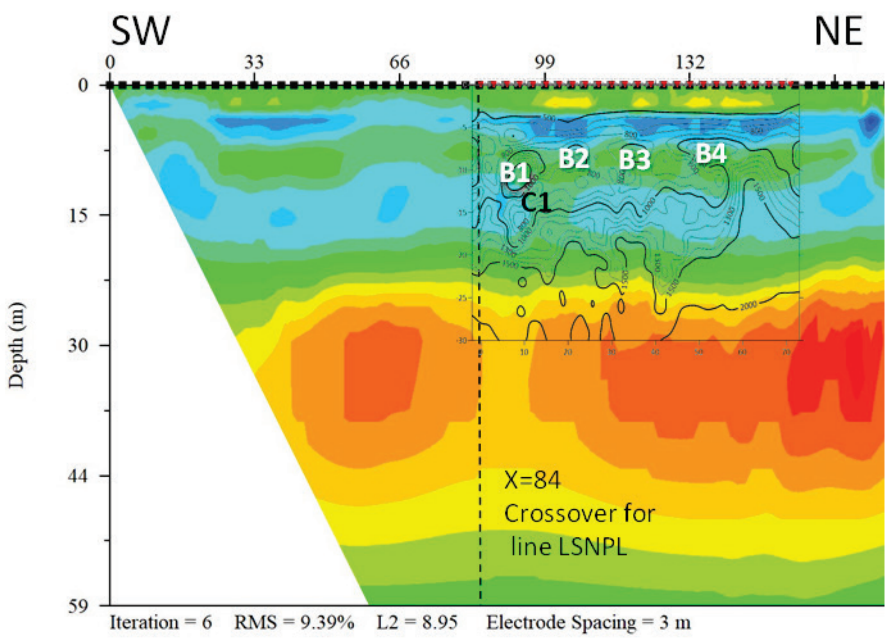

Figure 20. Overlay of seismic contours on southeast resistivity sections for (a) line LSSPL-1 and (b) line LSSPL-2. White lettering is used to represent relatively high seismic anomalies; black lettering represents relative low anomalies.

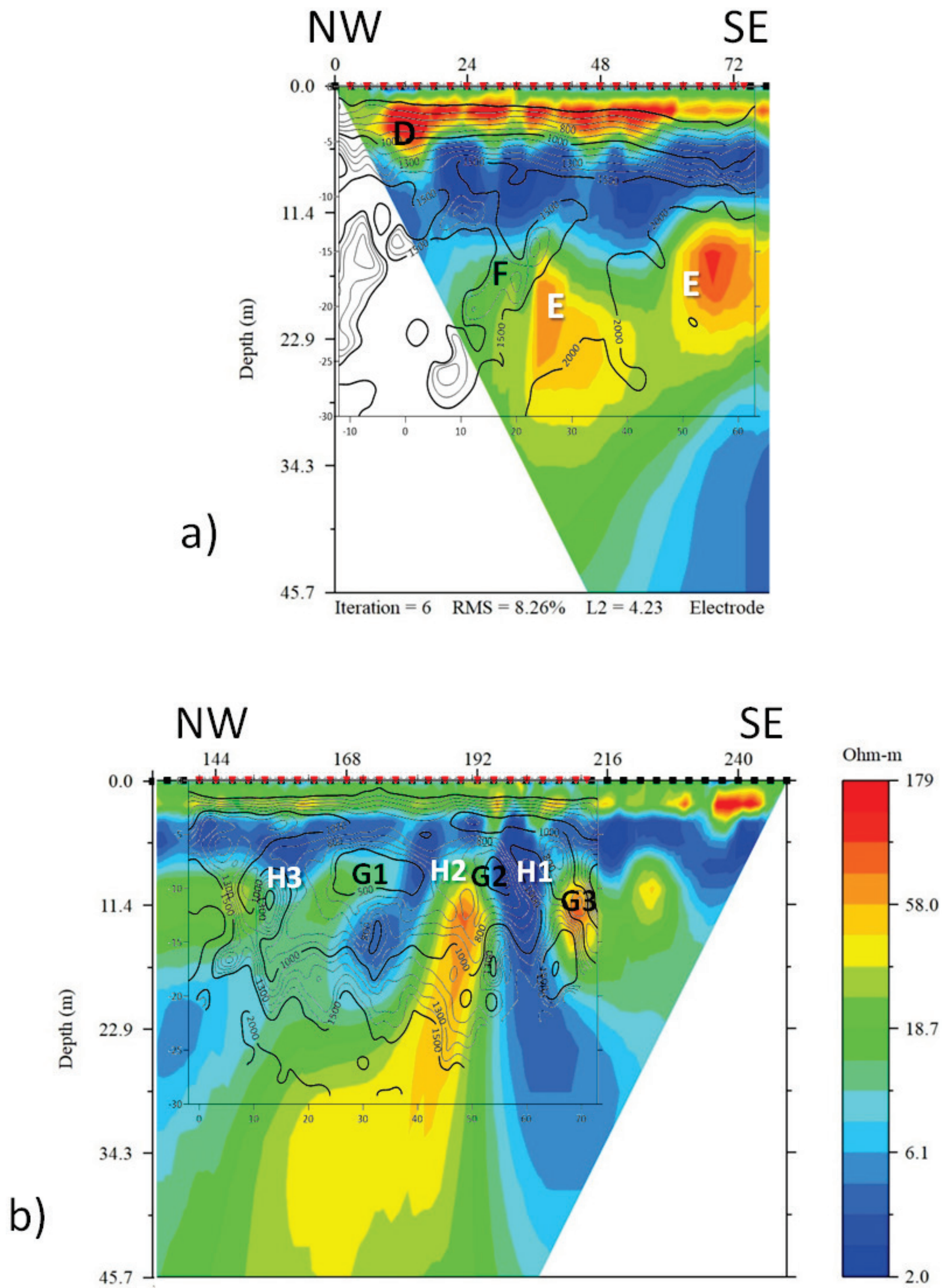

Figure 20 shows seismic lines LSSPL-1 and LSSPL-2 superimposed on the northwest and southeast ends, respectively, of resistivity line LSSPL. First, in comparing the portion corresponding to line LSSPL-1 (Figure 20a), the shallow 500 m/s seismic velocity contour does not match as well as on the north lines. Here it crosses a flat-lying high resistivity unit, dipping to the east (right), away from the river. The dip might be related to saturation where the water table would dip away from the river. Shallow velocity contours are quite regular here down to a depth of 7.0-8.0 m and a velocity of 1300-1400 m/s. The 1500 m/s contour falls in a low resistivity unit at a much shallower depth than where it occurred on the north side. There is a local deepening of the velocity contours at about 5.0-m depth on the northwest end of the line, identified as anomaly “D,” that corresponds with a thickening of the shallow, high resistivity (red) unit. This may be nothing more than an indication of poorer resolution near the end of both the seismic and resistivity lines. The shape of the 2000 m/s contour and the high velocity area represented by the two “E” anomalies corresponds with the deep high resistivity portion of the resistivity section. This is interesting because sands would have high resistivities but low velocities. Perhaps water content and/or saturation is playing a role in causing velocities to be relatively high. A low velocity feature, “F,” corresponds to an approximate west end of this feature and appears to continue upward into a portion of the low resistivity (blue) unit at 5.0- to 15.0-m depth.

Finally, in Figure 20b, seismic data from line LSSPL-2 are overlaid on the resistivity section. On this line, the 1000 m/s velocity contour corresponds with the top of a low resistivity layer at about 3.0-m depth, which is broken at about x=196.0 m above an underlying area that is more complicated than any of the other lines in the two areas. Here, in the resistivity section, three nearly vertical conductivity features are seen, alternating from low to high to low, and flanked by high resistivity features. This area is also the most complicated among the seismic lines, with alternating low velocity zones (G1, G2, and G3) separated by higher velocity zones (H1, H2, and H3). The velocities in the center of the low velocity zones are lower than similar features on other lines and occur on a line where the higher (>1000 m/s) seismic velocities occur shallower than on any of the other lines. In general, low velocity zones correspond reasonably well to high resistivities, and high velocity zones correspond with low resistivities. This could imply that the “G” anomalies are associated with sands while the “H” anomalies are associated with more clay-rich units. Of course, other interpretations for the low velocity areas, such as voids, are also possible. This area should be monitored for sinkhole, sand boils, or other activity that could compromise the performance of the Low Sill structure.

It is not surprising to find that both the seismic and resistivity sections correspond in some areas and are vastly different in others. Seismic methods are particularly sensitive to the strength of materials and their saturation. Resistivity will respond to the presence of electrically conductive minerals as well as the presence of pore fluids and their ionic properties, e.g., concentration of electrolytes, and pore connectivity. Both seismic and resistivity measurements will vary with seasonal changes in saturation.

7 Summary

A geophysical investigation was conducted in 2018 on both the northeast and southeast sides of the Low Sill structure as the first phase of a project to assess the condition of the grout and riprap volume at the structure. This is to include delineation of the boundaries of the grout body and riprap fill volume and identification of anomalies within the grout/riprap body that might be associated with voids or similar areas of concern. The purpose of the first phase was to identify structural features that might influence the long-term stability of the dam as well as to provide geological and geophysical context for pending water-borne geophysical surveys that are planned for spring or summer 2019, upstream and downstream of the structure. The two primary methods deployed were electrical resistivity and seismic refraction tomography. In addition, water-borne GPR data were acquired upstream of the structure in an exploratory study; however, because of the high water conductivity, no useable information was obtained.

A total of three resistivity lines and four shorter seismic lines were acquired within two study areas—one northeast and one southeast of the LSCS. Resistivity data indicate a relatively simple layered structure on the northeast side that correlates well with a geologic cross section constructed from available borehole information. On the southeast side, resistivity data show a layered subsurface except for a highly disturbed area within the eastern portion of the study area. Seismic data on the northeast side showed good correspondence in general with the resistivity data, though showing more variability in the seismic properties below depths of 5.0-10.0 m. The stratigraphy confirmed by both geologic profiles and geophysical surveys will contribute to a more accurate stability analysis of the structure. On the southeast side, an anomalous area was encountered in both resistivity and seismic data sets with similarly located alternating high/low anomalies at 5.0-20.0 m depth (Figure 21). These anomalies have features that are similar to those seen at sand boils or voids at other sites located in proximity to major rivers. This area should be monitored for sinkhole, sand boil, or other activity that could compromise the performance of the Low Sill structure.

Figure 21. Aerial view of the anomalous area that has been identified in resistivity data (line LSSPL) and seismic data (line LSSPL-2) in the southeast area. The resistivity line is shown in white, seismic line is shown in red, and the location of the anomaly is outlined in green.

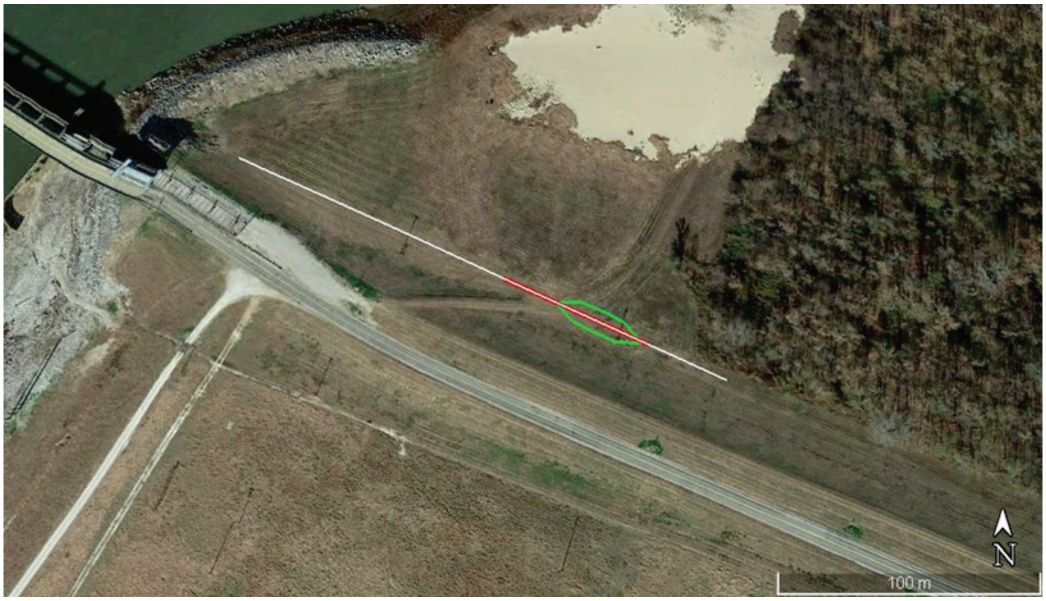

8 References

Fisk, H. N. 1947. *Fine-grained alluvial deposits and their effects on Mississippi River activity*. Vicksburg, MS: U.S. Army Engineer Waterways Experiment Station.

Heath, R. E., G. L. Brown, C. D. Little, T. C. Pratt, J. J. Ratcliff, D. D. Abraham, D. Perkey, N. B. Ganesh, K. Martin, and D. P. May. 2015. *Old River Control Complex sedimentation investigation*. ERDC TR-15-8. Vicksburg, MS: U.S. Army Engineer Research and Development Center.

Saucier, R. T. 1969. *Geological investigation of Mississippi River area Artonish to Donaldsonville, LA*. TR S-69-4. Vicksburg, MS: U.S. Army Engineer Waterways Experiment Station.

______. 1994. *Geomorphology and quaternary geologic history of the Lower Mississippi Valley*. Vol. I and II. Vicksburg, MS: U.S. Army Engineer Waterways Experiment Station.

U.S. Army Corps of Engineers (USACE). 1954. *Detailed design memorandum – low sill structure*. DM No. 4. Vicksburg, MS: U.S. Army Engineer Waterways Experiment Station.

U.S. Geological Survey (USGS). 2021. National Water Information System: Web interface. https://waterdata.usgs.gov/nwis/inventory?agency_code=USGS&site_no=310638091381401.

REPORT DOCUMENTATION PAGE

Form Approved OMB No. 0704-0188

1. REPORT DATE *(DD-MM-YYYY)*	2. REPORT TYPE	3. DATES COVERED *(From - To)*
September 2021	Final	

4. TITLE AND SUBTITLE

Geophysical Investigation to Assess Condition of Grouted Scour Hole:

Old River Control Complex—Low Sill Concordia Parish, Louisiana

5a. CONTRACT NUMBER

5b. GRANT NUMBER

5c. PROGRAM ELEMENT NUMBER

6. AUTHOR(S)

Janet E. Simms, Benjamin R. Breland, and William E. Doll

5d. PROJECT NUMBER

P2 110712

5e. TASK NUMBER

5f. WORK UNIT NUMBER

7. PERFORMING ORGANIZATION NAME(S) AND ADDRESS(ES)

Geotechnical and Structures Laboratory
U.S. Army Engineer Research and Development Center
3909 Halls Ferry Road
Vicksburg, MS 39180-6199

Oak Ridge Institute for Science and Education
P.O. Box 117
Oak Ridge, TN 37831-0117

8. PERFORMING ORGANIZATION REPORT NUMBER

ERDC/GSL TR-21-30

9. SPONSORING / MONITORING AGENCY NAME(S) AND ADDRESS(ES)

U.S. Army Corps of Engineers
New Orleans District
7400 Leake St.
New Orleans, LA 70118

10. SPONSOR/MONITOR'S ACRONYM(S)

11. SPONSOR/MONITOR'S REPORT NUMBER(S)

12. DISTRIBUTION / AVAILABILITY STATEMENT

Approved for public release; distribution is unlimited.

13. SUPPLEMENTARY NOTES

Funding provided by the sponsoring agency. Land-based and Water-borne Ground Penetrating Radar Surveys; Old River Low Sill Evaluation.

14. ABSTRACT

Geophysical surveys, both land-based and water-borne, were conducted at the Old River Control Complex–Low Sill, Concordia Parish, LA. The purpose of the surveys was to assess the condition of the grout within the scour region resulting from the 1973 flood event, including identification of potential voids within the grout. Information from the ground studies will also be used for calibration of subsequent marine geophysical data and used in stability analysis studies. The water-borne survey consisted of towed low frequency (16-80 MHz) ground penetrating radar (GPR), whereas the land-based surveys used electrical resistivity and seismic refraction. The GPR survey was conducted in the Old River Channel on the upstream side of the Low Sill structure. The high electrical conductivity of the water (~50 mS/m) precluded penetration of the GPR signal; thus, no useful data were obtained. The land-based surveys were performed on both northeast and southeast sides of the Low Sill structure. Both resistivity and seismic surveys identify a layered subsurface stratigraphy that corresponds, in general, with available borehole data and constructed geologic profiles. In addition, an anomalous area on the southeast side was identified that warrants future investigation and monitoring.

15. SUBJECT TERMS

Geophysics
Electrical resistivity
Mississippi River
Seismic refraction
Old River Control Complex
Low Sill
Concordia Parish (La.)
Diversion structures (Hydraulic engineering)
Grouting (Soil stabilization)
Geophysical surveys

16. SECURITY CLASSIFICATION OF:			17. LIMITATION OF ABSTRACT	18. NUMBER OF PAGES	19a. NAME OF RESPONSIBLE PERSON
a. REPORT	b. ABSTRACT	c. THIS PAGE			19b. TELEPHONE NUMBER *(include area code)*
Unclassified	Unclassified	Unclassified	SAR	43	